

Contents list available at CBIORE journal website

International Journal of Renewable Energy Development

Journal homepage: https://ijred.cbiore.id



Research Article

Optimized wind power prediction and energy storage scheduling using genetic algorithm and backpropagation neural network

Peng Wu nd Zongze Li*

Hebei Suntien New Energy Technology Co., Ltd., Zhangjiakou 075000, China

Abstract. As renewable energy continues to rise in the global energy mix, wind energy is gradually increasing its share in the power system as a clean, renewable form of energy. However, the volatility and uncertainty of wind power bring new challenges to power system operation, making the need for its efficient prediction and intelligent dispatch more and more urgent. Based on this, a method combining genetic algorithm and backpropagation neural network is proposed for wind power prediction and energy storage scheduling. In this study, the improved genetic algorithmbackpropagation algorithm was generated by optimizing the weights and thresholds of the backpropagation neural network through the genetic algorithm, and optimizing the crossover and mutation processes of the genetic algorithm using similar block-order single-point crossover operator and shift mutation operator. Moreover, the improved genetic algorithm-backpropagation Neural Network wind energy prediction model was successfully constructed. Subsequently, the improved genetic algorithm was applied to search for the parameters of support vector machine and an improved genetic algorithm-support vector machine photovoltaic power generation prediction model was established. The experimental results showed that the average absolute percentage error of the improved genetic algorithm backpropagation neural network algorithm was 2.4%, and the accuracy was significantly higher than that of the traditional backpropagation neural network algorithm. The maximum photovoltaic prediction error of the autoregressive integral moving average model was about 80MW, while the photovoltaic prediction error of the improved genetic algorithm support vector machine photovoltaic prediction model was only about 12kW. In addition, the average absolute percentage error of the improved genetic algorithm support vector machine photovoltaic prediction model was only 1.53%, which was only 0.2% higher than the support vector machine prediction model. This study not only improves the stability of the power grid but also provides a practical and feasible method for realizing the largescale application of clean energy, making a positive contribution to the sustainable development of the energy industry.

Keywords: Genetic algorithm, Backpropagation neural network, support vector machine, wind power prediction, energy storage scheduling



@ The author(s). Published by CBIORE. This is an open access article under the CC BY-SA license (http://creativecommons.org/licenses/by-sa/4.0/).

Received: 5th June 2024; Revised: 27th Oct 2024; Accepted: 6th Dec 2024 Available online: 21th Dec 2024

1. Introduction

Currently, the power system is undergoing a profound transformation from traditional energy sources to renewable energy sources. While the use of renewable energy sources, including wind power (WP), has significantly lessened the impact on the environment, its unpredictability and intermittency complicate power system operation and planning (Gurhanli 2020; Saravi et al. 2021; Yang et al. 2021). In this context, wind power prediction (WPP) has become an important part of solving the problem of WP volatility. Traditional mathematical models and algorithms perform poorly in handling the complex nonlinear relationships of WTG output. Many traditional models are based on linear assumptions and cannot effectively capture the complex nonlinear relationship between wind speed and WP output. Meanwhile, traditional algorithms rely heavily on historical data and lack flexibility. When data is scarce or of poor quality, the predictive power of the model is significantly reduced. There is a significant gap in the existing research in the field of WPP, especially in terms of model flexibility, adaptability, and accuracy. Therefore, there is an urgent need to explore more advanced methods to improve the performance of WPP to better meet the needs of the power system. On the other hand, genetic algorithm (GA) can enhance the adaptability of WPP model by simulating biological evolution and globally searching the parameter space (Kshirsagar *et al.* 2021). Backpropagation (BP) neural network, on the other hand, can accurately capture the effect of wind speed (WS) variation on WP output by learning historical data patterns (Dawid and Kopel, 2019). For a result, combining GA and BP and using GA to optimize the BP network parameters can enhance the prediction model's capacity for generalization even further.

With the challenges posed by the rapid growth of renewable energy sources, especially the volatility of wind energy, researchers have worked on the development of WPP techniques and energy storage scheduling (ESS) strategies. Through advance knowledge of WP volatility trends and intelligent energy storage (ES) system scheduling, the aim is to optimize power system operation and improve the efficiency of renewable energy utilization while ensuring system stability and reliability. Keynia and Memarzadeh (2022) proposed a method based on the combination of WP production, tariff and financial gain/loss (FLG) forecasting with ES, aiming to address the

^{*} Corresponding author Email: lizongze19940321@163.com (Z.Li)

forecasting and scheduling challenges posed by the uncertainty of WP generation with wind. The experimental results indicated that with this method, the expected profit could be improved by 4.44-27.69% in a given forecast month by adjusting the initial offer based on the FLG forecast. Wan found that the intermittency and volatility of WP posed a great threat to the safety of power system operation, and proposed a control scheme based on probability prediction. This method combined probabilistic WPP with multivariate Gaussian copula to generate time-dependent WP scenarios. Simultaneously, the adaptive variational mode decomposition method was used to extract frequency components. The results showed that this method could effectively reduce the fluctuation of WP (Wan et al., 2021). Semero et al., (2020) proposed an optimal unit commitment and dispatch model for distributed generation in the grid in a grid-connected microgrid system. The model aimed to optimize ES equipment and combined heat and power (CHP) generating units through load and renewable generation forecasts to minimize the overall system operating costs. Simulation results revealed that optimal scheduling of ES system and CHP units using this strategy could significantly reduce the system operating costs. Li and Chen (2019) proposed an optimal control strategy for wind farms with battery ES system centered on an optimal control model. The strategy aimed to minimize the number of battery energy storage system (BESS) orders, taking into account statistical control effects and battery ES system operational constraints, including charging states and dead zones. Simulation results demonstrated that the control strategy reduced the number of BESS orders while improving the accuracy of the WP tracking plan, and had an anti-interference function to prevent the ultra-short-time WPP error. Martinez Rico et al., (2020) proposed a hybrid renewable energy system optimization method based on energy arbitrage to address the randomness and intermittency issues of renewable energy sources such as wind and solar power. This method utilized storing energy at low electricity prices and selling it at high electricity prices to maximize the profit of the power plant and reduce the loss of battery value. By fitting the particle swarm optimization algorithm to solve the multiobjective cost function, the results showed that considering energy efficiency significantly improved battery life, while profitability was similar to not considering value loss. Xia et al., (2020) proposed a multi period coordinated scheduling model to address the power balance challenges posed by intermittent renewable energy sources such as WP and photovoltaics. The model was divided into three time scales: day ahead scheduling, one hour ahead scheduling and 15 minutes ahead scheduling. The simulation results showed that the model effectively utilized the regulation capabilities of different power generation methods, successfully tracked changes in active power, and achieved the economic operation of the system. Liu et al., (2023) proposed an energy optimization scheduling method for distribution networks with a source load storage aggregation group to address the energy imbalance caused by large-scale distributed generation access. First, a system model of the distribution network layer and the SAGs layer was established, and then a load forecasting method based on Adaboost integrated convolutional neural network and bidirectional long short-term memory was adopted. The simulation results verified the accuracy of the load forecasting model and the effectiveness of the proposed optimization strategy in energy optimization scheduling.

On the other hand, BP is able to capture more accurately the effect of WS changes on WP output by learning complex patterns in historical data. Many scholars launched a series of

researches on it. Scholars such as Wright et al., (2022) proposed a method based on direction propagation algorithm for the training problem of deep neural networks. The process analyzed the execution efficiency of the neural network in the classification task using different physics techniques, and added expandable modules to the method. Experimental results demonstrated that the proposed method had good training efficiency. Leung et al., (2023) proposed a BP based method for the problem of signal timing logic analysis. The research process used a systematic approach to transform robust formulas, utilized computational graphs and automatic differentiation tools to complete the BP, and added gradient methods for integration. Experimental results indicated that the proposed method had a wide range of applicability. Park and Lee (2022) proposed a method based on BP algorithm for the problem of stereo matching. The process maintained the spatial resolution, adjusted the number of parallax planes, and excluded the large difference pixels between the real ground parallax. According to experimental data, the suggested approach offers a high accuracy for stereo matching. Khehra et al., (2022) have proposed a technique based on BP algorithm for the problem of x-ray image classification. The process could preset the possible image types of x-ray images, statistical texture features are extracted and the performance of the technique is analyzed using accuracy. According to the findings, the suggested strategy had a high categorization efficiency. Colak (2021) proposed an assistive technique based on BP algorithm for the research problem of nanofluids. The process utilized experimental data as a data source, incorporated multilayer perfusers in the network structure and calculated the thermal conductivity. The findings demonstrated the effectiveness of the suggested strategy in connecting the experimental findings.

In conclusion, while WPP and ESS research is currently advancing at a rapid pace, several challenges remain. These include the unpredictability of wind energy, which is difficult to fully eliminate, and the optimization of ES system capacity and efficiency. To achieve the comprehensive development of intelligent renewable energy applications, further in-depth research is necessary (Fan et al., 2024; Graça Gomes et al., 2021; Muttagi and Sutanto, 2021). On the other hand, GA simulates biological evolution and globally searches the parameter space to optimize the WPP model, which can improve the adaptability. BP can accurately capture the impact of WS changes on WP output by learning historical data patterns (Li and Li, 2020). Therefore combining the two, GA optimizes the BP network parameters, which can make the prediction model more generalized and perform better in WPP (Nikoobakht et al., 2020; Xue et al., 2022; Watabe et al., 2021). Based on this, the study proposes a WPP with ESS method that fuses GA with BP neural network. At the same time, in response to the problem of long computation time for WPP, the study introduced similar block order single point and code shift mutation to optimize the crossover and mutation process of GA, and proposed an improved genetic algorithm (IGA). First, the BP was optimized by IGA, and by modifying the initial weights and thresholds, the WPP model of GA-BP was effectively built. Then, the GA was used to determine the Support Vector Machine (SVM) kernel function parameters and penalty factor, and finally, the IGA-SVM Photovoltaic (PV) power generation prediction model was built. The innovation of the research is to fully combine GA with BP neural network, and optimize the initial weights and thresholds of BP neural network. Meanwhile, the crossover and mutation process of GA was optimized, and an IGA based on similar block order single point and code shift burst was proposed to construct an efficient WPP model. The IGA was

applied to optimize the penalty factor and kernel function parameters of SVM, and an ESS model was successfully constructed. This novel algorithm can achieve higher accuracy and efficiency in actual WPP and ESS. Compared with existing methods, the model proposed in this study has been deeply optimized for the accuracy of WP generation prediction and can better adapt to the volatility of WP generation. At the same time, the combination of algorithm efficiency and prediction models is more flexible, which can effectively improve the economic operation efficiency of the system. In addition, the IGA-SVM photovoltaic power generation prediction model created by the research is beneficial for further improving the scheduling capabilities.

This study consists of five parts. The first part presents the research background, problems, and solutions related to WPP and ESS. The second part reviews the previous research results on WPP and ESS, and summarizes the difficulties and shortcomings of the methods. The third part presents the improvement of BP algorithm by combining GA. To compare the effectiveness of the new method with the traditional method, a comparison experiment is designed in the fourth part. The fifth part summarizes the research method, analyzes the experimental results, and puts forward the shortcomings and prospects of the method.

2. Wind Power Prediction and Energy Storage Scheduling Method Based on BP

In order to increase prediction accuracy, this study investigates the joint usage of BP and GA to optimize the WPP model's parameters through GA and BP further training. In the meantime, in order to accomplish the goals of increasing the power system's dispatchability and lowering operating costs, the GA is introduced to improve the scheduling strategy of the ES system by achieving the synergistic operation of WP and ES.

2.1 GA Improved BP Prediction Method Design

WP energy prediction is to analyze and simulate the meteorological conditions, such as WS and direction, of a WP site for a certain period of time in the future through the use of techniques such as meteorology, statistics and machine learning, in order to predict the power generation energy of the WP system (Garai *et al.*, 2023; Hebbi and Mamatha, 2023; Kim *et al.*, 2020). The WS will directly effect the wind turbine (WT)'s power because the fundamental idea of wind energy is that the wind turns mechanical energy into electrical energy through the WT's rotation and then through the generator (Bandewad *et al.*, 2023). Equation (1) provides the mathematical expression for the power of a WT. The most significant parameters influencing a WT's power output are its features and the WS.

$$p = \frac{1}{2} \cdot \rho \cdot C_P \cdot A \cdot v^3 \tag{1}$$

In equation (1), p denotes the output power of the WT (kW) and ρ denotes the air density (kg/m3). C_P indicates the power coefficient of the WT, and A indicates the swept area of the WT (m²). v is the WS (m/s). Equation (1) states that the fan power is directly proportional to the air density. Since temperature and air pressure also have an impact on air density, equation (2) provides a quantitative expression for air density.

$$\rho = 3.48 \frac{p_q}{T} \left(1 - 0 \cdot 387 \frac{\varphi p_b}{p_q} \right) \tag{2}$$

In equation (2), p_q denotes the standard atmospheric pressure (kPa) and φ denotes the relative humidity of the air (%rh). p_b is the saturated water vapor pressure (kPa) and T is the thermodynamic temperature of air (K). Turbulence is a common phenomenon in nature p_b and reflects the change in WS. WTs are affected by turbulence, which affects the full utilization of wind energy. Therefore, it is crucial to study the effect of turbulence on WT power. The mathematical expression for the turbulence intensity I_T is given in equation (3).

$$I_T = \frac{\sigma}{V} \tag{3}$$

In equation (3), σ denotes the standard deviation of WS (m/s) and V is the average WS (m/s). The WPP deviates from the actual value and cannot be completely 100% accurate. BP is a multilayer feed forward neural network that minimizes the output error at a given input through learning and training (Gomes *et al.*, 2020; Guo *et al.*, 2020). The study uses BP for network correction to minimize the error until the desired accuracy is achieved. Figure 1 illustrates the BP structure.

The input layers (IL), hidden layers (HL), and output layers (OL) of the BP network in Figure 1 are made up of linked neurons. The input signal is processed to produce an output value in the OL and the error is calculated by comparing it with the desired output. The weights and thresholds are adjusted between neurons by error BP and the network is modified to reduce the error until the desired accuracy is achieved (El Bourakadi *et al.*, 2022; Zhu *et al.*, 2022). The first information is transmitted by the IL, and the activation function is a constant function. Equation (4) displays the expression for the buried layer's activation function, which is the tansig function.

$$f(x) = \frac{2}{1 + e^{-2x}} - 1 \tag{4}$$

In equation (4), *e* denotes the Euler number. Equation (5) provides the expression for the logsig function, which is used as the activation function in the OL.

$$f(x) = \frac{1}{1 + e^{-x}} \tag{5}$$

The input signal of a BP network introduces a certain amount of systematic error as it is passed layer by layer through the HL, IL, and OLs. By passing the error in the reverse direction, this process is repeated so that the error gradually satisfies a specific condition (Xing *et al.*, 2022). The definition expression of the systematic error E is detailed in equation (6).

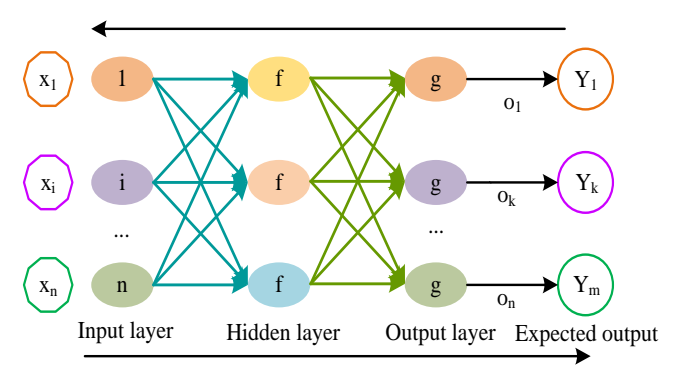


Fig. 1 Structure diagram of BP neural network

$$E = \sum_{k=1}^{num} |d_k - y_k| \tag{6}$$

In equation (6), num denotes the total amount of training data, d_k denotes the expected value, and y_k denotes the output value. The BP network algorithm consists of two stages: forward propagation and BP. In forward propagation, the input expression of the j th node of the HL is shown in equation (7).

$$input_{j=} \sum_{i=1}^{x} u_{ji} x_i + y_j \tag{7}$$

In equation (7), x_i denotes the input value of the IL, y_j denotes the deviation value of the implied layer, and u_{ji} denotes the connection weights between the nodes of the IL and implied layers. Equation (8) displays the expression for the implicit layer's jth node's output value.

$$out_i = f(input_i) = f(\sum_{i=1}^{x} u_{ii} x_i + y_i)$$
(8)

In equation (8), out_j denotes the output value of the jth node of the implicit layer. The input of the kth node of the OL is shown in equation (9).

$$input_k = \sum_{j=1}^q v_{kj} C_j + b_k = \sum_{j=1}^n v_{kj} f(\sum_{i=1}^n u_{ji} x_i + y_j) + b_k$$
 (9)

In equation (9), f(x) denotes the transfer function of the implicit layer, v_{kj} denotes the weights between the nodes of the implicit layer and OL, and b_k denotes the OL node threshold. Where $i=1,2,3,\ldots,n$, $j=1,2,3,\ldots,q$, $k=1,2,3,\ldots,m$. Equation (10) displays the output value of the OL's kth node.

$$O_k = g(input_k) = g(\sum_{j=1}^q v_{kj}C_j + b_k) = g(\sum_{j=1}^q v_{kj}f)$$

$$(\sum_{i=1}^n u_{ii}x_i + a_i) + b_k$$
(10)

In equation (10), g(x) denotes the transfer function of OL and O_k is the output of the OL node. a_j denotes the deviation value of the hidden function. The standard algorithm for network weight adjustment is based on the error gradient descent method. To begin, the precise computation in equation (11) is

applied by computing the error table between each sample's actual and intended output.

$$E_p = \frac{1}{2} \sum_{k=1}^{num} (T_k - O_k)^2 \tag{11}$$

In equation (11), T_k represents the intended result. Reducing the error function is the aim of network training. Error BP's primary task is to update the weights and thresholds in order to minimize error. To make sure the weights and thresholds meet the requirements, the network is trained repeatedly. Figure 2 depicts the BP-based WPP method.

The steps involved in using BP in WPP are shown in Figure 2, where the error between the output and the predicted value is calculated, the error BP is used to update the weights and thresholds, and the error is reduced by iterative training. The initial weights and thresholds of BP are usually chosen randomly within a certain range, but improper selection may lead to problems. GA can be used to determine the optimal initial weights and thresholds to increase prediction accuracy and prevent the local minimum problem. Firstly, the derivative of the systematic error E is defined as the meta-adaptation function. Equation (12) displays the mathematical expression as well.

$$f = a \frac{1}{F} \tag{12}$$

In equation (12), *a* denotes the coefficient. Selection, crossover and mutation, and looping are carried out until the computation is finished once the fitness function has been established. In addition, the GA-BP neural network algorithm has the problem of long computation time when predicting WP. In response to this issue, research has optimized the crossover, mutation, and local search stages of the GA. The effectiveness of the GA method largely depends on the population initialization process, and the selection of crossover and mutation, as well as the probability of their adoption, will also greatly affect the effectiveness of the algorithm. Therefore, the study adopts an operator called similar block order single-point crossover to optimize the GA method. This operator first considers at least two consecutive blocks with the same order, and only the same blocks occupying the same position in the

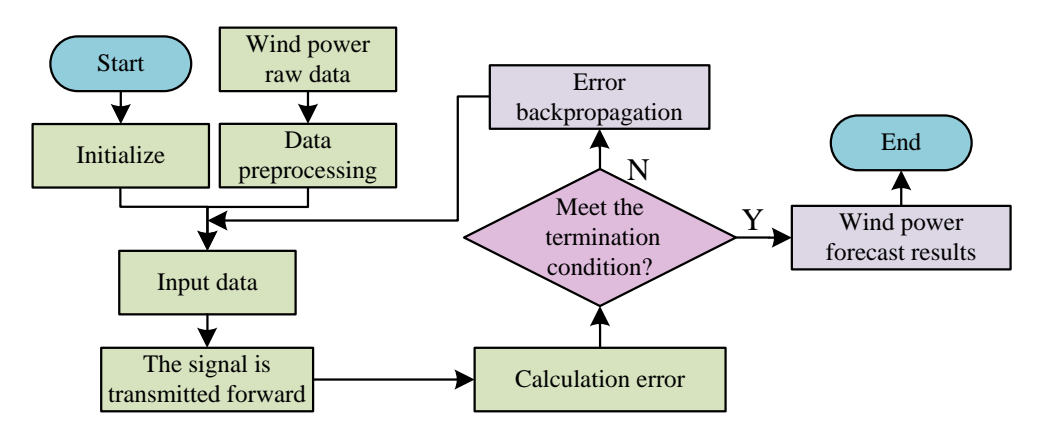


Fig. 2 Wind power prediction flow diagram based on BP neural network

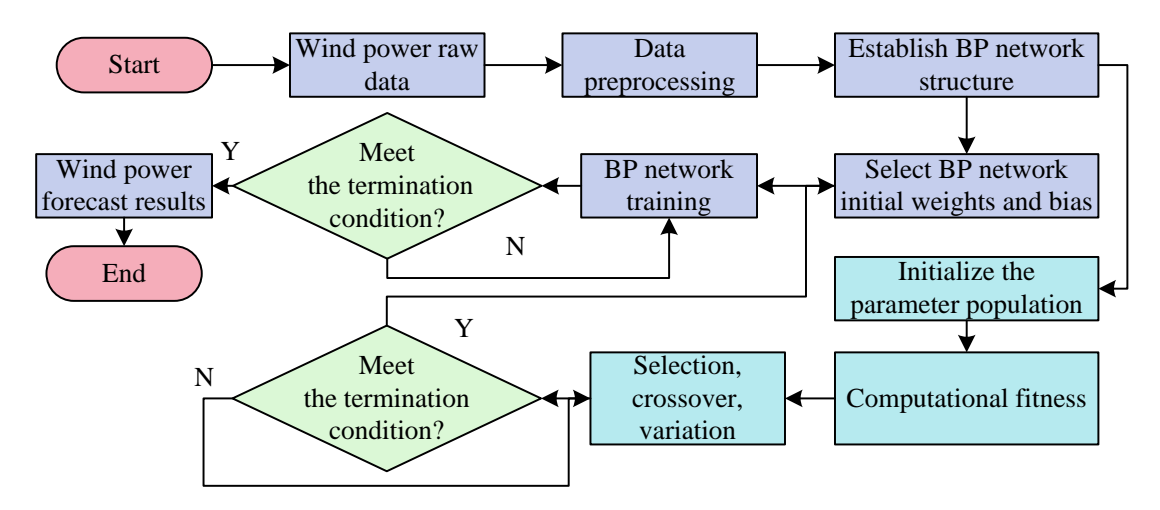


Fig. 3 Flow chart of WPP based on IGA-BP network

parent are directly copied to the child. Then, based on maintaining the same blocks, a single-point sequential crossover method is used to cross the parent. In addition, in the selection of mutation operators, the study selected shift mutation, which randomly selects a workpiece to be inserted in another random position. Similar block order single-point crossover operators and shift mutation operators can better utilize information in the population and reduce unnecessary computation, which can solve the problem of long computation time to some extent. Figure 3 illustrates the flowchart of the IGA-BP algorithm based WPP.

First, to improve the model's initial performance, Figure 3 illustrates how IGA optimization is applied to set the weights and thresholds of the first BP. The weights and thresholds are then continuously adjusted using the error BP approach to reduce the difference between the expected and actual values and, ultimately, produce correct WPP. The BP is then employed for training. Photovoltaic power prediction utilizes existing and past PV output data through modeling in order to obtain future PV power. Figure 4 depicts the battery's performance at various irradiance levels at a standard temperature of 25°C. Solar irradiance is a measure of the energy of solar radiation that reaches the earth's surface.

In Figure 4, under constant temperature conditions, Figure 4(a) clearly demonstrates the trend of increasing the current of the photovoltaic cell as the irradiance is enhanced. Correspondingly, Figure 4(b) shows that the output power of the

photovoltaic cell also tends to increase with increasing irradiance, which in turn leads to a corresponding change in the maximum power point of the photovoltaic cell.

2.2 Energy Scheduling of Energy Storage System Based on IGA Optimized SVM

Autoregressive integrated moving average model (ARIMA) is a method for dealing with non-stationary time series that combines regression, differencing and moving average (Bali *et al.*, 2020; Lochmann *et al.*, 2023). Differencing is one of the key steps, which can improve the stability of the series, but too much differencing may lead to information loss. The loss of information needs to be minimized while maintaining the stability of the series. PV forecasting based on the ARIMA model starts with the processing of the time series, which is formulated in equation (13).

$$\nabla x_t = x_t - x_{t-1} = (1 - B)x_t \tag{13}$$

In equation (13), B denotes the delay factor, $\nabla = 1 - B$ denotes the ordered difference operator of the incoming, and the expression of the time series after order difference is shown in equation (14).

$$\nabla^d x_t = (1 - B)^d x_t \tag{14}$$

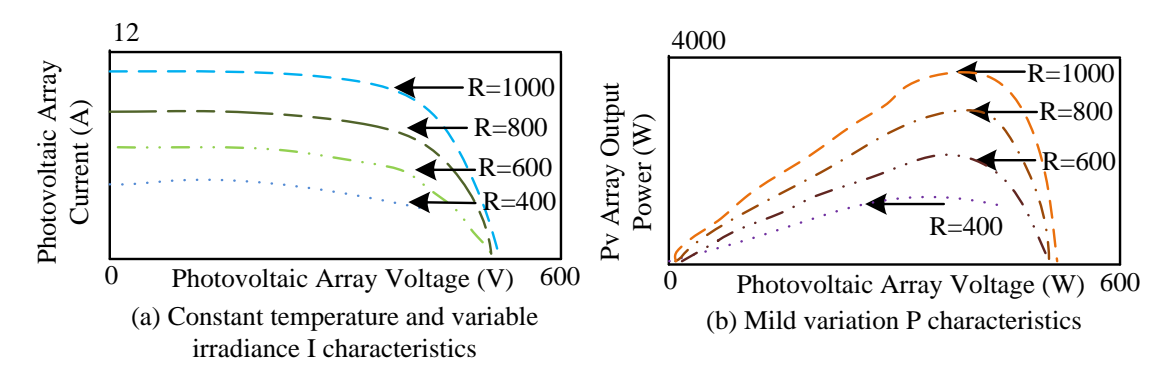


Fig. 4 Characteristic change curve of photovoltaic cells (constant temperature)

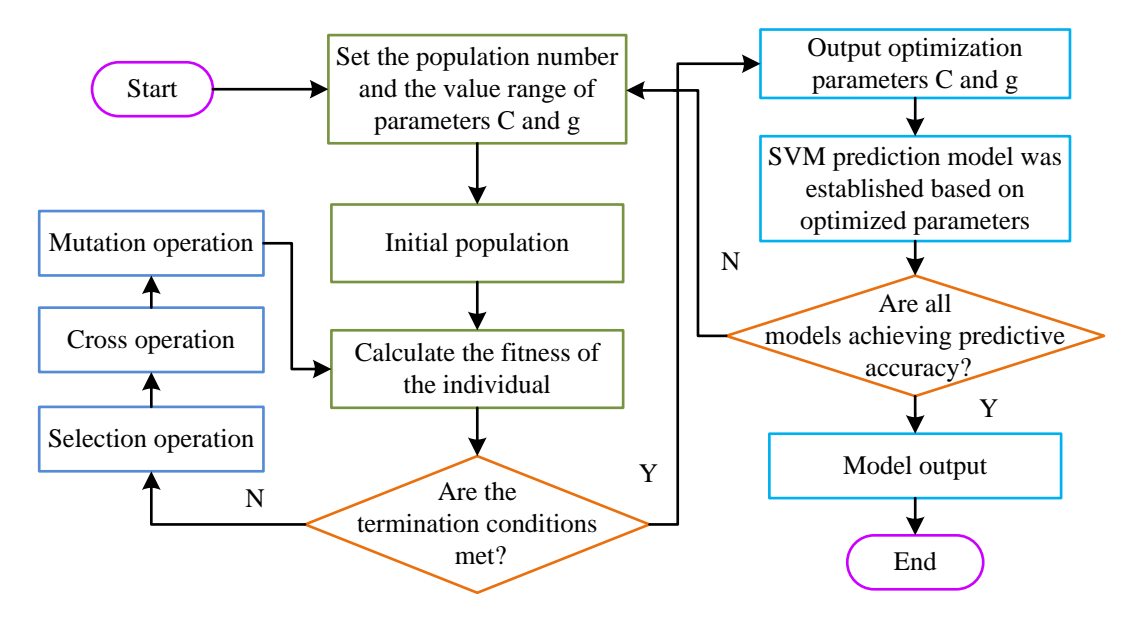


Fig. 5 IGA-SVM prediction model flow chart

In equation (14), d denotes the number of differences. B denotes the delay operator and $\nabla=1$ —B denotes the introduced ordered difference operator. After the time series processing, the next step is to perform model identification. In order to select the model that matches the sequence $\{x_t\}$, the autocorrelation function (ACF) and partial autocorrelation function (PACF) of the sequence can be utilized for model identification. After determining the sequence model type, the appropriate n and m values need to be selected. Usually, the Information criterion function method is used to determine the model order, while in the study, Akaike information criterion (AIC) is chosen to be used for the model order determination. In equation (15), the precise mathematical formula is also displayed.

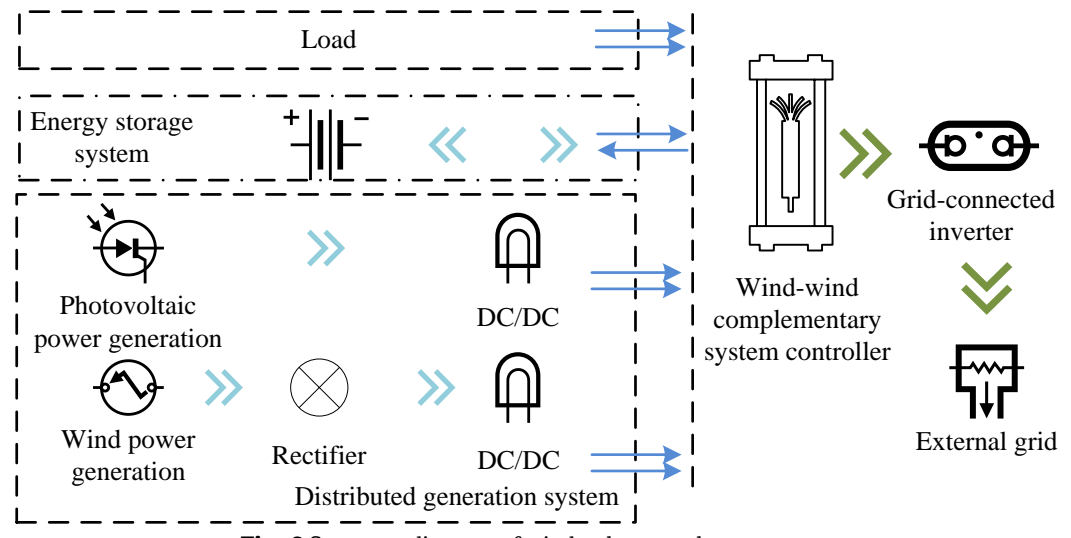
$$AIC = 2k - 21n(L) \tag{15}$$

In equation (15), k and L denote the number of model parameters and the great likelihood function, respectively.

Finally, the parameter estimation is carried out, and the study obtains the PV power generation prediction model based on ARIMA. The study uses the IGA to optimize the SVM model, taking the kernel function parameter g and the penalty factor C as the optimization-seeking object to construct the IGA-SVM prediction model (Chen $et\ al.$, 2022; Patil $et\ al.$, 2021; Sun $et\ al.$, 2024). The IGA-SVM prediction model's flow chart is displayed in Figure 5.

In Figure 5, first, the optimal kernel function type and parameters are selected by IGA. Subsequently, the trained SVM model is utilized to predict the test data. The final goal of the entire procedure is to maximize SVM performance and raise prediction accuracy through IGA by assessing the model's performance and making the required modifications.

The complimentary nature of solar and wind energy is fully utilized by the wind and solar power generation system, which can increase power supply stability and dependability. The system is categorized into off-grid and grid-connected types. The off-grid type is mainly used for microgrid, supplying



 $\textbf{Fig. 6} \ \textbf{Structure diagram of wind-solar complementary system}$

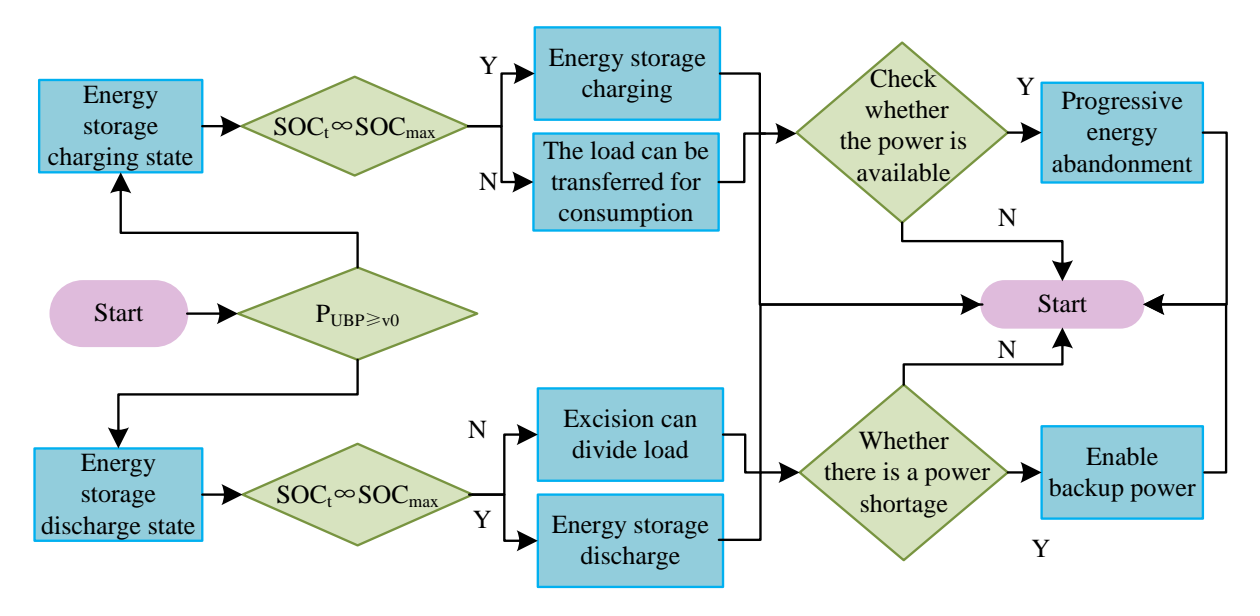


Fig. 7 Energy management strategy flow chart

electricity to the load and storing the excess electricity. The grid-connected type can be connected to a large power grid to realize self-generation, self-consumption and on-grid connection of surplus electricity. Figure 6 shows the system components.

In Figure 6, the wind-solar complementary system includes several main parts such as solar PV battery bank, WT, ES system, grid-connected inverter, and system controller. The inconsistent energy output of the new energy grid-connected presents difficulties for the wind-solar hybrid system. To solve this problem, the research focuses on establishing a wind-solar ES system. Combining wind and PV power forecasting models, the optimal ES plan is finally obtained using IGA. Figure 7 illustrates the energy management strategy flow.

In Figure 7, the ES system enters the charging state when the wind energy produces excess power. If the charging power is within the constraints, the system continues to charge. However, if the constraints are exceeded, the ES approaches the upper limit of charging and the adjustable load consumes the excess energy to balance the energy difference between time periods. Conversely, if there is not enough wind and solar energy to generate power, the ES enters the discharge state. If the exported power is sufficient to make up the shortfall, the

system discharges. However, if the constraints are exceeded, the ES approaches the lower limit of discharge and some of the load must be removed. When the adjustable load reaches the maximum regulation and there is still a shortfall, the back-up power is activated.

3. Performance Validation of BP-Based Wind Power Prediction and Energy Storage Scheduling

Comparative tests are designed to validate the prediction accuracy performance of the IGA-BP approach with the classic BP network, with the aim of thoroughly validating its adaptability and generalization ability. Additionally, by contrasting the discretization of the IGA-SVM PV prediction model with the SVM prediction model, the study validates the model's performance. This series of comparative experiments aims to comprehensively assess the effectiveness of the proposed method and ensure that its performance under different conditions is fully validated.

3.1 Performance Validation of IGA-Improved BP Prediction Method

To further validate the performance of the IGA-BP neural network algorithm, experiments are conducted using the

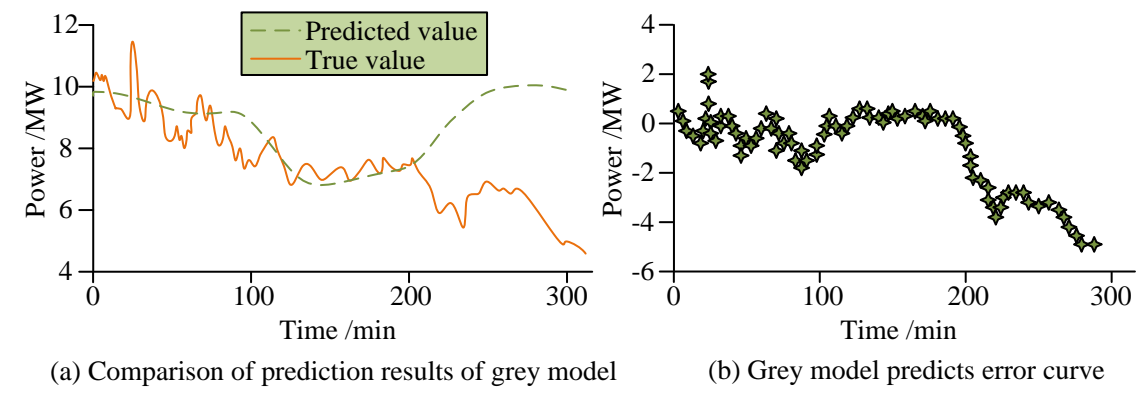


Fig. 8 Prediction error curve of grey model and comparison of prediction results with BP neural network prediction of random samples

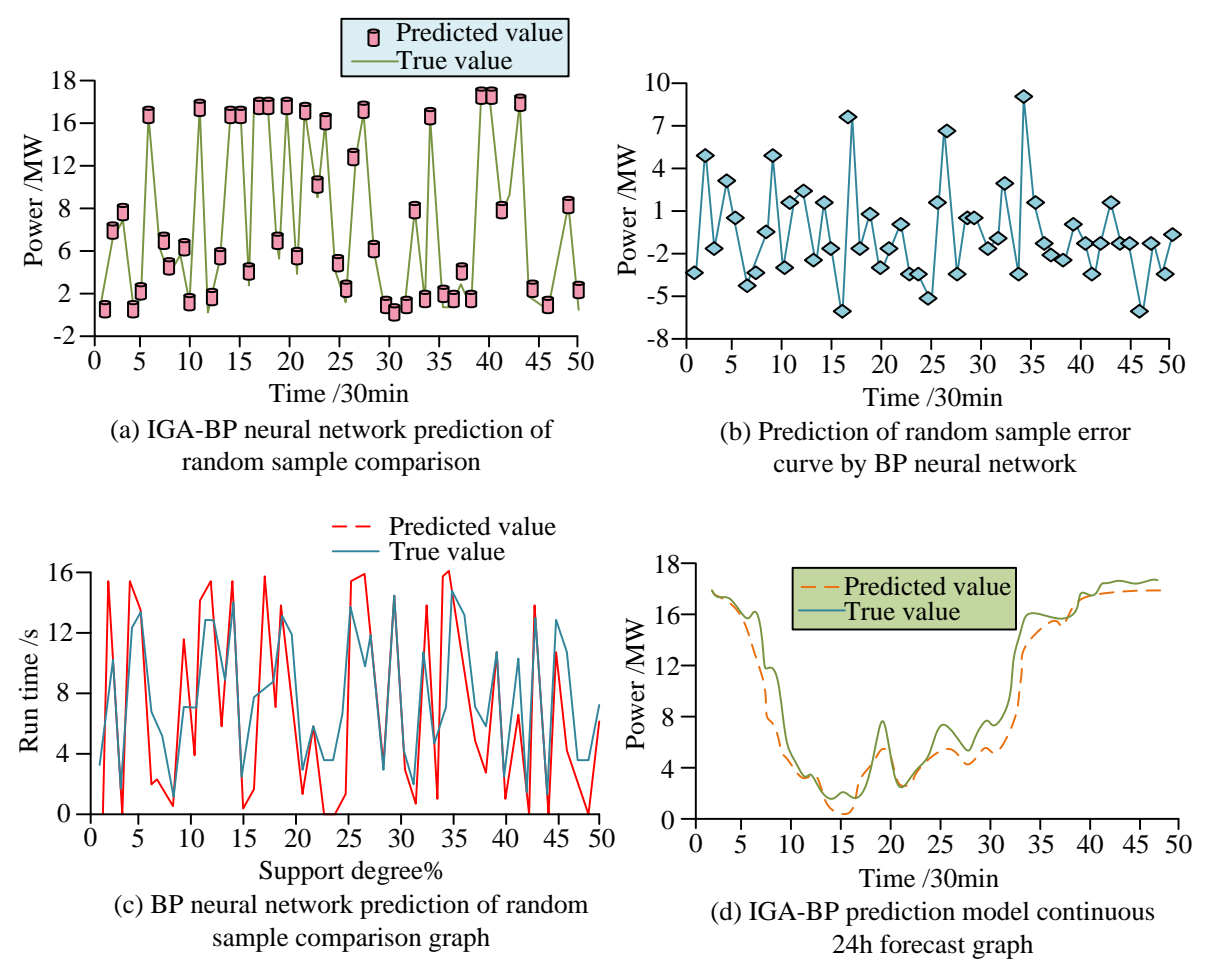


Fig. 9 Comparison of BP and IGA-BP neural network prediction of random samples, BP neural network error curve of random samples, and IGA-BP prediction model prediction graph for 24h

Table 1

1 abic 1	
Name	Environmental parameters
Processor	Intel(R) Core(TM) i5-9500 CPU @ 3.00 GHz
System type Memory	64 bit operating system 16GB
Software environment	MATLAB 2020a

Table 2

Parameter	Value
Population size	50
Iterations	50
Cross probability	0.8
Mutation probability	0.2
Learning rate	0.001

measured WP data of a wind farm for the entire year of 2022. The wind farm used is located in Shandong Province, which has become an important area for WP development due to its superior wind resources and suitable climate conditions. A total of 3534 samples are collected and divided into training and testing sets in an 8:2 ratio. Among them, the training set contains 2827 samples, the test set consists of 707 samples. The simulation environment is shown in Table 1.

The parameter settings for the IGA are shown in Table 2. To verify the effectiveness of the IGA-BP-WPP model, the study sets up a comparison experiment to compare the errors of the gray WPP model, the traditional BP-WPP model and the IGA-BP proposed in the study. Figure 8 demonstrates the gray model prediction error curve compared with the prediction results.

In Figure 8(a), the color model's prediction results are more accurate for the first 200 minutes or so. However, beyond that time, the prediction value steadily increases while the real value steadily drops. The two do not overlap, indicating a poor prediction performance. In Figure 8(b), in the first 200 min or so, the prediction error fluctuates above and below 0 MW, and after 200 min, the prediction error shows a decreasing trend, reaching a minimum of about -5 MW. The study further records the random sample comparison of neural network prediction of BP and IGA-BP, the random sample error curve of BP, and the continuous 24h prediction of IGA-BP prediction model, which are shown in Figure 9.

In Figure 9(a), the IGA-optimized IGA-BP is more consistent with the test data, and the accuracy is significantly improved despite the long computation time. In Figure 9(b), the traditional BP improves the prediction accuracy, but the error is still significant. In Figure 9(c), the BP predicts a smaller difference in comparison of random samples, but there is still an error. In Figure 9(d), the training effect of the model random samples is supported by the good fit between the prediction and actual curves. To evaluate the accuracy improvement of the prediction

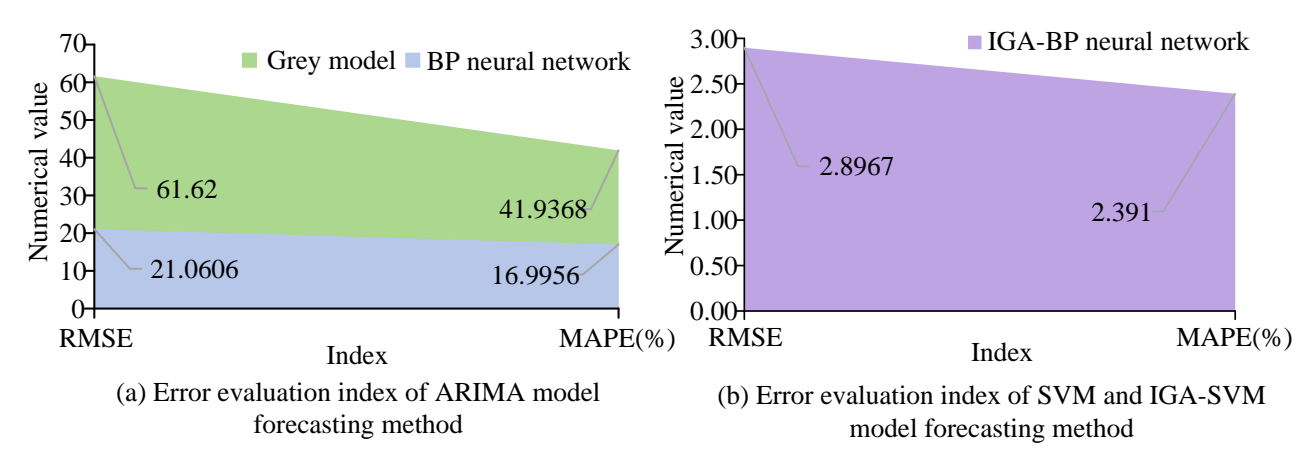


Fig. 10 Comparison of error evaluation indexes of the three forecasting methods

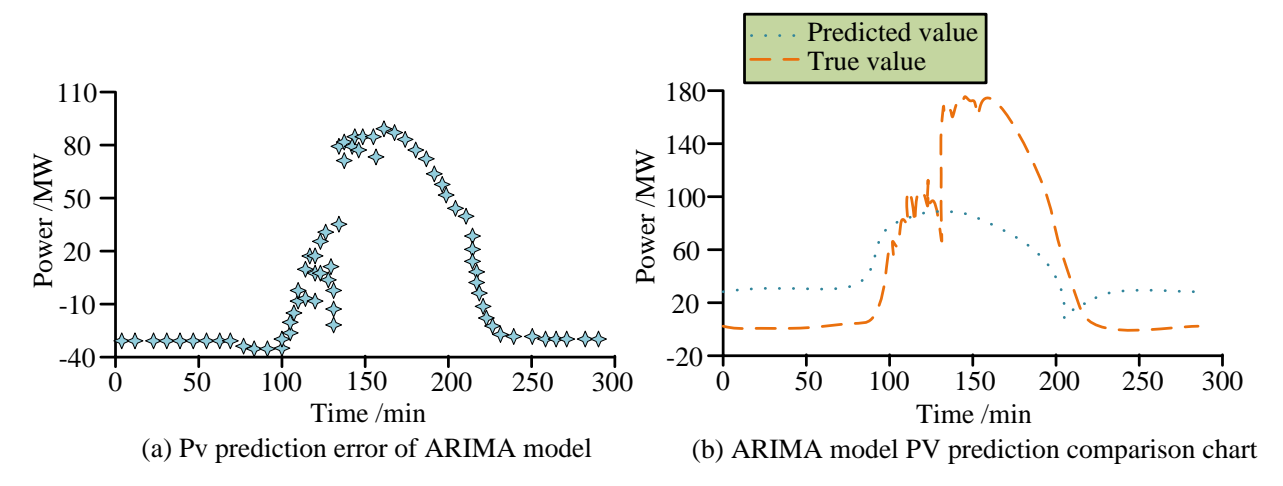


Fig. 11 Comparison of prediction results and error curve of ARIMA PV prediction model

algorithm in this study, Figure 10 compares the error assessment indices of the three prediction techniques.

Figure 10(a) shows that the gray model's average absolute percentage error is 41.9368 and its root mean square error is 61.62. Figure 10(b) shows that the accuracy of the IGA-BP method is greatly improved, with an average absolute percentage error of 2.4%. Overall, the improved BP with IGA exhibits a stronger WPP capability.

3.2 Performance Validation of IGA-SVM based Photovoltaic Prediction Models

The study configured the IGA with a population size of 50, 50 iterations, a crossover probability, and a variance probability of 4 to 1. The contrast between the error curve and the ARIMA PV prediction model's prediction outcomes is shown in Figure 11.

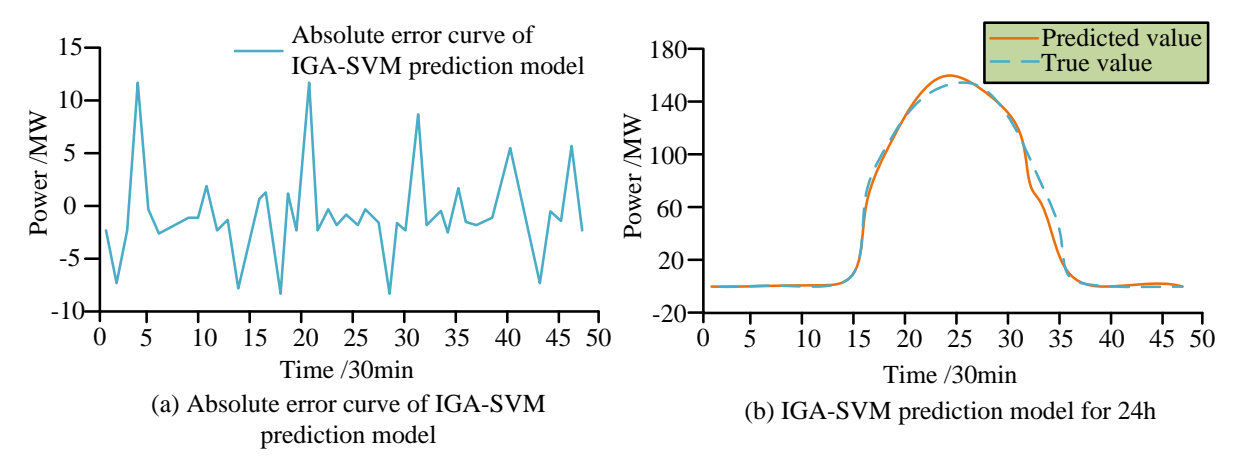


Fig. 12 Absolute error curve of IGA-SVM prediction model and prediction results for 24

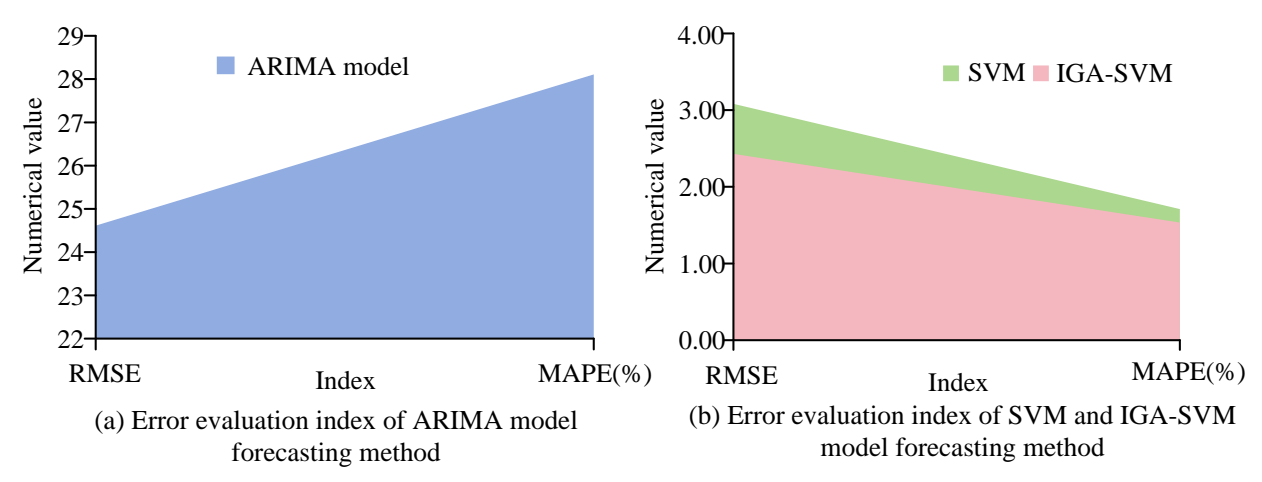


Fig. 13 Comparison of error evaluation indexes of the three forecasting methods

According to Figure 11(a), the ARIMA PV prediction error is up to about 80 MW. Figure 11(b) shows that there is a significant discrepancy between the true value and the anticipated value of the ARIMA model PV forecast, with the difference getting closer only at about 120 minutes. Taken together, the ARIMA PV prediction model has a large error and cannot be used directly in PV prediction. Figure 12 records the absolute error curve of IGA-SVM prediction model with continuous 24h prediction results

The maximum inaccuracy of the IGA-SVM is approximately 12 kW, as shown in Figure 12(a). The reduced error fluctuation range of the suggested model indicates that the IGA-SVM PV prediction model is more stable and accurate. The IGA-SVM prediction model essentially matches the true value in the continuous 24-hour prediction, as shown by Figure 12(b), indicating a greater prediction accuracy. To further confirm the effectiveness of the proposed IGA-SVM PV prediction model in the study, Figure 13 compares the error evaluation indices of the three prediction strategies.

In Figure 13(a), the RMSE of the ARIMA model is around 24.6 and the MAPE is around 28%. According to Figure 13(b), the MAPE is around 1.5%. The IGA-SVM PV prediction model has an average absolute percentage error of 1.53%, which is just 0.2% more than the SVM prediction model. It is noteworthy that the degree of dispersion in the outcomes produced by the IGA-SVM PV prediction model is lower.

4. Discussion

To verify the effectiveness of the IGA-BP neural network WPP model, the grey WPP model, the traditional BP neural network WPP model, and the proposed IGA-BP neural network were compared for errors. The results showed that the prediction results of the grey model were close to the true values in the first 200 minutes, but showed poor prediction performance after 200 minutes. The root mean square error of the model was 61.62, and the average absolute percentage error was 41.9368. Although traditional BP neural networks improved their prediction accuracy, the errors were still significant. The predicted data from the IGA-BP neural network was more consistent with the true values. The average absolute percentage error of this algorithm was only 2.4%. The reason was that the IGA-BP neural network combined IGA to optimize the weights and biases of the BP neural network, which could effectively avoid the problem of the BP neural network getting stuck in local optimal solutions during training. In addition, the IGA-BP neural network had stronger adaptability in dealing with the nonlinear and time-varying characteristics in WPP. Zhang et al., (2022) proposed the IGA-BP algorithm to address the problem of inaccurate alcohol content detection in segmented wine picking. The results showed that the average prediction error of this method for alcoholic beverages was 0.381, which was significantly better than the traditional BP neural network. To verify the superiority of the IGA-SVM photovoltaic prediction model, it was compared with the ARIMA photovoltaic prediction model. The results showed that the ARIMA photovoltaic prediction error was as high as about 80MW, and the predicted value differed significantly from the true value, with a MAPE of about 28%. The MAPE of the IGA-SVM photovoltaic prediction model was only 1.53%, and compared with the SVM prediction model, the error only increased by 0.2%. The IGA-SVM model used the IGA to optimize SVM, which enabled the model to explore the parameter space more effectively when selecting support vectors and adjusting hyperparameters. At the same time, the method optimized the selection of input features, which could screen out the most influential features for photovoltaic power generation prediction, fully explore the potential patterns in photovoltaic power generation data, and significantly reduce the prediction error. Huang et al., (2023) applied the IGA SVM algorithm to the classification of agricultural products. The results showed that the classification accuracy of the algorithm was as high as 98%. This indicated that the algorithm had significant advantages in feature selection, nonlinear processing, global optimization, and adaptability, which made it perform well in areas such as photovoltaic prediction and agricultural product classification.

However, the study did not consider the impact of factors such as climate change, load demand fluctuations, and policy changes on ESS. Meanwhile, research on ESS mainly focuses on economic benefits without fully analyzing the volatility of output power. Future research should comprehensively analyze various potential factors in the modeling process, especially in the field of ESS. It is recommended to introduce research on power fluctuation suppression to improve the stability and adaptability of the system.

5. Conclusion

As the proportion of wind energy in the power system increases, the demand for accurate prediction of WP and smart ES rises sharply. However, traditional methods are difficult to meet the nonlinearity and time-varying nature of WP, and improving WPP accuracy has become a top priority. This study explored the combined application of IGA and BP to optimize the WPP model parameters by IGA and then use BP for further training, with a view to improving the prediction accuracy. Meanwhile, the IGA was introduced to optimize the scheduling strategy of the ES system, by realizing the cooperative operation of WP and ES. The experimental results indicated that the error was significantly reduced to 2.4% when using the IGA-BP algorithm for WPP, which was an improvement of about 14.5% compared to 16.9% for the traditional BP network. This algorithmic improvement resulted in a significant increase in WPP accuracy. The SVM prediction model demonstrated a high degree of consistency over 24 consecutive hours, and the predicted values were in good agreement with the true values. This progress has profound implications for practical applications, especially in renewable energy and power systems. Accurate WPP can not only optimize power scheduling and enhance the integration capability of renewable energy, but also effectively improve the scheduling strategy of intelligent energy storage systems, thus achieving the coordinated operation of WPP and energy storage. At the same time, this research is beneficial for promoting the wider application of clean energy and supporting the construction of sustainable power systems. However, it has limitations as other influencing factors were not fully considered in the modeling process. In the study of ES energy scheduling, researchers have primarily focused on economic benefits without fully considering output power volatility. Future studies should comprehensively analyze various potential factors in the modeling process, particularly in ES energy scheduling, where it is necessary to include the study of suppressing power fluctuation to improve the system's robustness and stability.

Numenclature

Municipalature	
Abbreviation	Full name
WP	Wind power
WPP	Wind power prediction
GA	Genetic algorithm
BP	Backpropagation
ESS	Energy storage scheduling
IGA	Improved genetic algorithm
ES	Energy storage
SVM	Support vector machine
FLG	Tariff and financial gain/loss
BESS	Battery energy storage system
ARIMA	Autoregressive integrated moving average model
WT	Wind turbine
IL	Input layers
HL	Hidden layers
OL	Output layers
PV	Photovoltaic

Author Contributions: Peng Wu collected the samples. Zongze Li analysed the data. Peng Wu and Zongze Li conducted the experiments and analysed the results. All authors discussed the results and wrote the manuscript.

Funding: The author(s) received no financial support for the research, authorship, and/or publication of this article.

Conflicts of Interest: The authors report that no conflict interests.

References

Bali, V., Kumar, A., & Gangwar, S. (2020). A novel approach for wind speed forecasting using LSTM-ARIMA deep learning models. International Journal of Agricultural and Environmental Information

- Systems (IJAEIS), 11(3), 13-30; https://doi.org/10.4018/IJAEIS.2020070102
- Bandewad, G., Datta, K. P., Gawali, B. W., & Pawar, S. N. (2023). Review on discrimination of hazardous gases by smart sensing technology. Artificial Intelligence and Applications, 1(2): 86-97; https://doi.org/10.47852/bonviewAIA3202434
- Chen, Y., Zhou, Z., Yang, L., Hu, G., Han, X., & Tang, S. (2022). A novel structural safety assessment method of large liquid tank based on the belief rule base and finite element method. *Proceedings of the Institution of Mechanical Engineers, Part O: Journal of Risk and Reliability*, 236(3), 458-476; https://doi.org/10.1177/1748006X211021690
- Colak, A. B. (2021). Experimental study for thermal conductivity of water-based zirconium oxide nanofluid: Developing optimal artificial neural network and proposing new correlation. *International Journal of Energy Research*, 45(2), 2912-2930; https://doi.org/10.1002/er.5988
- Dawid, H., & Kopel, M. (2019). On economic applications of the genetic algorithm: A model of the cobweb type. *Journal of Evolutionary Economics*, 8(3), 297-315; https://doi.org/10.1007/s001910050066
- El Bourakadi, D., Yahyaouy, A., & Boumhidi, J. (2022). Improved extreme learning machine with AutoEncoder and particle swarm optimization for short-term wind power prediction. *Neural Computing and Applications*, 34(6), 4643-4659; https://doi.org/10.1007/s00521-021-06619-x
- Fan, B., Liao, F., Yang, C., & Qin, Q. (2024). Two-stage electricity production scheduling with energy storage and dynamic emission modelling. *International Journal of Production Research*, 62(18), 6473-6492; https://doi.org/10.1080/00207543.2023.2280186
- Garai, S., Paul, R. K., Kumar, M., & Choudhury, A. (2023). Intra-annual national statistical accounts based on machine learning algorithm. *Journal of Data Science and Intelligent Systems*, 2(2), 12-15; https://doi.org/10.47852/bonviewJDSIS3202870
- Gomes, I. L. R., Melício, R., Mendes, V. M. F., & Pousinho, H. M. (2020).
 Wind power with energy storage arbitrage in day-ahead market by a stochastic MILP approach. *Logic Journal of the IGPL*, 28(4), 570-582; https://doi.org/10.1093/jigpal/jzz054
- Graça Gomes, J., Telhada, J., Xu, H., Sá da Costa, A., & Zhao, C. (2021). Optimal operation scheduling of a pump hydro storage system coupled with a wind farm. *IET Renewable Power Generation*, *15*(1), 173-192; https://doi.org/10.1049/rpg2.12014
- Guo, T., Zhu, Y., Liu, Y., Gu, C., & Liu, J. (2020). Two-stage optimal MPC for hybrid energy storage operation to enable smooth wind power integration. *IET Renewable Power Generation*, 14(13), 2477-2486; https://doi.org/10.1049/iet-rpg.2019.1178
- Gurhanli, A. (2020). Accelerating convolutional neural network training using ProMoD backpropagation algorithm. *IET Image Processing*, 14(13), 2957-2964; https://doi.org/10.1049/iet-ipr.2019.0761
- Hebbi, C., & Mamatha, H. (2023). Comprehensive dataset building and recognition of isolated handwritten kannada characters using machine learning models. *Artificial Intelligence and Applications*, 1(3), 179-190; https://doi.org/10.47852/bonviewAIA3202624
- Huang, L., Chen, Y., Wang, J., Cheng, Z., Tao, L., Zhou, H., Xu, J., Yao M., Liu, M., & Chen, T. (2023). Online identification and classification of Gannan navel oranges with Cu contamination by LIBS with IGA-optimized SVM. *Analytical Methods*, 15(6): 738-745; https://doi.org/10.1039/d2ay01874h
- Keynia, F., & Memarzadeh, G. (2022). A new financial loss/gain wind power forecasting method based on deep machine learning algorithm by using energy storage system. *IET Generation, Transmission & Distribution, 16*(5), 851-868; https://doi.org/10.1049/gtd2.12332
- Khehra, B. S., Pharwaha, A. P. S., Jindal, B., & Mavi, B. S. (2022). Classification of clustered microcalcifications using different variants of backpropagation training algorithms. *Multimedia Tools and Applications*, 81(12), 17509-17526; https://doi.org/10.1007/s11042-022-12017-9
- Kim, J., Kwon, D., Woo, S. Y., Kang, W. M., Lee, S., Oh, S., Kim, C. H., Bae, J. H., Park, B. G., & Lee, J. H. (2020). Hardware-based spiking neural network architecture using simplified backpropagation algorithm and homeostasis functionality. *Neurocomputing*, 428(38), 153-165; https://doi.org/10.1016/j.neucom.2020.11.016
- Kshirsagar, P. R., Manoharan, H., Tirth, V., Naved, M., Siddiqui, A. T., & Sharma, A. K. (2021). Automation monitoring with sensors for

- detecting covid using backpropagation algorithm. KSII Transactions on Internet and Information Systems, 15(7), 2414-2433; https://doi.org/10.3837/tiis.2021.07.007
- Leung, K., Aréchiga, N., & Pavone, M. (2023). Backpropagation through signal temporal logic specifications: Infusing logical structure into gradient-based methods. *The International Journal of Robotics Research*, 42(6), 356-370; https://doi.org/10.1177/02783649221082115
- Li, B., & Chen, B. (2019). Rolling optimal control strategy with lead control for wind power and energy storage systems. *Dianli Xitong Zidonghua/Automation of Electric Power Systems*, 43(4), 25-32; https://doi.org/10.7500/AEPS20180302002
- Li, M., & Li, Y. (2020). Dispatch planning of a wide-area wind power-energy storage scheme based on ensemble empirical mode decomposition technique. *IEEE Transactions on Sustainable Energy*, 12(2), 1275-1288; https://doi.org/10.1109/TSTE.2020.3042385
- Liu, K., Sheng, W., Li, Z., Liu, F., Liu, Q., Huang, Y., & Li, Y. (2023). An energy optimal schedule method for distribution network considering the access of distributed generation and energy storage. *IET Generation, Transmission & Distribution*, 17(13), 2996-3015; https://doi.org/10.1049/gtd2.12855
- Lochmann, M., Kalesse-Los, H., Schäfer, M., Heinrich, I., & Leinweber, R. (2023). Analysing wind power ramp events and improving very short-term wind power predictions by including wind speed observations. *Wind Energy*, *26*(6), 573-588; https://doi.org/10.1002/we.2816
- Martinez-Rico, J., Zulueta, E., de Argandoña, I. R., Fernandez-Gamiz, U., & Armendia, M. (2020). Multi-objective optimization of production scheduling using particle swarm optimization algorithm for hybrid renewable power plants with battery energy storage system. *Journal of Modern Power Systems and Clean Energy*, *9*(2), 285-294; https://doi.org/10.35833/MPCE.2019.000021
- Muttaqi, K. M., & Sutanto, D. (2021). Adaptive and predictive energy management strategy for real-time optimal power dispatch from VPPs integrated with renewable energy and energy storage. *IEEE Transactions on Industry Applications*, 57(3), 1958-1972; https://doi.org/10.1109/TIA.2021.3057356
- Nikoobakht, A., Aghaei, J., Shafie-Khah, M., & Catalão, J. P. S. (2020). Minimizing wind power curtailment using a continuous-time risk-based model of generating units and bulk energy storage. *IEEE Transactions on Smart Grid*, 11(6), 4833-4846; https://doi.org/10.1109/TSG.2020.3004488
- Park, J. M., & Lee, J. W. (2022). Improved stereo matching accuracy based on selective backpropagation and extended cost volume. *International Journal of Control, Automation and Systems*, 20(6), 2043-2053; https://doi.org/10.1007/s12555-021-0724-6
- Patil, A. P., Mishra, B. K., & Harsha, S. P. (2021). Fault diagnosis of rolling element bearing using autonomous harmonic product spectrum method. *Proceedings of the Institution of Mechanical Engineers, Part K: Journal of Multi-body Dynamics*, 235(3), 396-411; https://doi.org/10.1177/1464419321994986
- Saravi, V. S., Sakhaei, H., Kalantar, M., & Anvari-Moghaddam, A. (2021).

 A novel power management strategy based on combination of 3D

- droop control and EKF in DC microgrids. *IET Renewable Power Generation*, 15(11), 2540-2555; https://doi.org/10.1049/rpg2.12187
- Semero, Y. K., Zhang, J., & Zheng, D. (2020). Optimal energy management strategy in microgrids with mixed energy resources and energy storage system. *IET Cyber-Physical Systems: Theory & Applications*, 5(1), 80-84; https://doi.org/10.1049/iet-cps.2019.0035
- Sun, J., Li, H., Yao, Y., & Dong, F. (2024). Research on the identification of the production origin of Angelica dahurica using LIBS technology combined with machine learning algorithms. *Optoelectronics Letters*, 20(3), 171-176; https://doi.org/10.1007/s11801-024-3114-5
- Wan, C., Qian, W., Zhao, C., Song, Y., & Yang, G. (2021). Probabilistic forecasting based sizing and control of hybrid energy storage for wind power smoothing. *IEEE Transactions on Sustainable Energy*, 12(4), 1841-1852; https://doi.org/10.1109/TSTE.2021.3068043
- Watabe, M., Shiba, K., Chen, C. C., Sogabe, M., & Sogabe, T. (2021). Quantum circuit learning with error backpropagation algorithm and experimental implementation. *Quantum Reports*, 3(2), 333-349; https://doi.org/10.3390/quantum3020021
- Wright, L. G., Onodera, T., Stein, M. M., Wang, T., Schachter, D. T., Hu, Z., & McMahon, P. L. (2022). Deep physical neural networks trained with backpropagation. *Nature*, 601(7894), 549-555; https://doi.org/10.1038/s41586-021-04223-6
- Xia, S., Ding, Z., Du, T., Zhang, D., Shahidehpour, M., & Ding, T. (2020). Multitime scale coordinated scheduling for the combined system of wind power, photovoltaic, thermal generator, hydro pumped storage, and batteries. *IEEE Transactions on Industry Applications*, 56(3), 2227-2237; https://doi.org/10.1109/TIA.2020.2974426
- Xing, Z., Qu, B., Liu, Y., & Chen, Z. (2022). Comparative study of reformed neural network based short-term wind power forecasting models. *IET Renewable Power Generation*, 16(5), 885-899; https://doi.org/10.1049/rpg2.12384
- Xue, X., Ai, X., Fang, J., Cui, S., Jiang, Y., Yao, W., Chen, Z., & Wen, J. (2022). Real-time schedule of microgrid for maximizing battery energy storage utilization. *IEEE Transactions on Sustainable Energy*, 13(3), 1356-1369; https://doi.org/10.1109/TSTE.2022.3153609
- Yang, B., Zeng, C., Wang, L., Guo, Y., Chen, G., Guo, Z., Chen, Y., Li, D., Cao, P., Shu, H., Yu, T., & Zhu, J. (2021). Parameter identification of proton exchange membrane fuel cell via Levenberg-Marquardt backpropagation algorithm. *International Journal of Hydrogen Energy*, 46(2), 22998-23012; https://doi.org/10.1016/j.ijhydene.2021.04.130
- Zhang, J. H., Shang, J. W., Wang, C., Zhao, Y., Li, K. X., & Li, X. L. (2022).
 Research on alcohol prediction model based on LSTM and IGA-BP.
 Food and Machinery, 38(5), 71-77;
 https://doi.org/10.13652/j.spjx.1003.5788.2022.90072
- Zhu, T., Wang, W., & Yu, M. (2022). Short-term wind speed prediction based on FEEMD-PE-SSA-BP. *Environmental Science and Pollution Research*, 29(52), 79288-79305; https://doi.org/10.1007/s11356-022-21414-4



© 2025 The Author(s). This article is an open access article distributed under the terms and conditions of the Creative Commons Attribution-ShareAlike 4.0 (CC BY-SA) International License (http://creativecommons.org/licenses/by-sa/4.0/)